Optical and Structural Characterization of Epitaxial Nanoporous GaN Grown by CVD

Optical and Structural Characterization of Epitaxial Nanoporous GaN Grown by CVD.

Josué Mena[1], Joan J. Carvajal [1,*], Oscar Martínez [2], Juan Jiménez [2], Vitaly Z. Zubialevich[3], Peter J. Parbrook[3,4], Francesc Diaz[1], Magdalena Aguiló[1]

[1] Física i Cristal·lografia de Materials i Nanomaterials (FiCMA-FiCNA) and EMaS, Dept. Química Física i Inorgànica, Universitat Rovira i Virgili (URV), Tarragona, Spain

[2] GdS-Optronlab group, Dpto. Física de la Materia Condensada, Univ. de Valladolid, Valladolid, Spain

[3] Tyndall National Institute, Lee Maltings, Dyke Parade, Cork, Ireland

[4] School of Engineering, University College Cork, Cork, Ireland

Abstract

In this paper we study the optical properties of nanoporous GaN epitaxial layers grown by CVD on non-porous GaN substrates, using photoluminescence, cathodoluminescence, and resonant Raman scattering, and correlate them with the structural characteristic of these films. We pay special attention to the analysis of the residual strain of the layers and the influence of the porosity in the light extraction. The nanoporous GaN epitaxial layers are under tensile strain, although the strain is progressively reduced as the deposition time and the thickness of the porous layer increases, becoming nearly strain free for a thickness of 1.7 μm. The analysis of the experimental data point to the existence of vacancy complexes as the main source of the tensile strain.

Introduction

The unique optoelectronic properties of gallium nitride (GaN) have motivated the fabrication of advanced devices, e.g. light emitting diodes (LEDs) [1], laser diodes [2], and microelectronic devices such as high electron mobility transistors (HEMTs), gas sensors [3] and GaN surface functionalized HEMT biosensors [4]. Generally, the GaN structures used to fabricate these devices are epitaxially grown on foreign substrates, e.g., *c*-oriented sapphire (α-Al_2O_3), and silicon carbide (6H-SiC). However, the lattice mismatch of these substrates with GaN is important, -13% and 4%, respectively [5], resulting in a high density of threading dislocations ($\sim 10^8$-10^{10} cm^{-2}), micro cracks and other extended defects such as stacking faults, voids, inversion domains, plus a significant amount of point defects [6].

The lattice mismatch, and the difference in the thermal expansion coefficients between GaN and foreign substrates, induce either compressive (on *c*-oriented sapphire substrates, for instance) or tensile (on 6H-SiC substrates) biaxial strains in the GaN epitaxial layers. The strain tensor components (ε) are similar on the *c*-plane and different along the perpendicular component, corresponding to the hexagonal symmetry of wurtzite GaN ($\varepsilon_{xx} = \varepsilon_{yy} \neq 0$, $\varepsilon_{zz} \neq 0$) [7]. Not only the built-in biaxial strain plays a role in the resulting strain of the layers, but also the point defects can induce local hydrostatic strain for which all the strain tensor components are equal ($\varepsilon_{xx} = \varepsilon_{yy} = \varepsilon_{zz}$) [7]. The hydrostatic strain is related to the difference between the atomic radius of the impurity or defect and the host atom replaced, it can be compressive or tensile [8]. As a consequence of the different strain contributions, the band structure, and, in particular, the band gap of GaN is modified, inducing a red-shift of the band-edge luminescence emission for tensile strain and a blue-shift when compressive strain prevails [9, 10]. Therefore, luminescence spectroscopy can be used to measure the strain in the GaN layers by means of the energy shift of the near band edge (NBE) emission [7]. Raman scattering is also a powerful and direct technique to monitor the residual strain in epitaxial GaN layers [11, 12]. The E_2(high) mode is highly sensitive to biaxial strain in III-nitrides. Under conventional visible excitation (non-resonant), the Raman spectrum of GaN can be masked by the Raman spectrum arising from the substrate; therefore, in order to selectively excite the top GaN layers, UV excitation is necessary, thus working under resonant conditions,

which introduces relevant changes in the spectrum. Under these conditions, the polar A_1(LO) mode allowed for backscattering on the (0001) plane is dramatically enhanced due to the Fröhlich interaction [13, 14]. Instead, the non-polar E_2(high) mode is not enhanced and it appears very weak because of the small scattering volume with UV excitation.

Porous GaN has been particularly interesting for the LED technology, since it shows higher light extraction efficiency, with respect to non-porous GaN, due to the multiple reflections on the lateral walls of the pores [15]. Porous GaN has been classically fabricated following a top-down approach based on photo-electrochemical [16] and chemical etching methods [17] of GaN epitaxial layers grown on foreign substrates. We have developed a bottom-up approach to fabricate homoepitaxial nanoporous layers of GaN in one single step by chemical vapour deposition (CVD) [18]. The growth of nanoporous GaN particles on Si substrates catalytically assisted by a metallic film, resulting in a polycrystalline film of porous particles randomly distributed [19], was reported in former works. These nanoporous GaN polycrystalline films were demonstrated to form low resistivity Ohmic contacts with high work function metals such as Au or Pt [20]. Also the growth of unintentionally doped *n*-type [18] and Mg-doped *p*-type [21] nanoporous GaN with pores oriented perpendicular to the substrate was achieved using (0001) GaN/sapphire substrates, allowing the growth of a fully porous *p*-*n* junction [22].

In this paper, we analyze the optical and structural properties of homoepitaxial nanoporous GaN layers grown in a single step by CVD on non-porous GaN deposited on sapphire substrates, paying special attention to the role played by the layer porosity on the residual strain through the luminescence emission. Experimental results obtained by photoluminescence (PL), resonant Raman scattering, and cathodoluminescence (CL), reveal the existence of tensile strain for low deposition times (resulting in porous layer thickness below ~1 μm). These characterization techniques have been used in the past to analyse the structural strain encountered in porous GaN layers prepared by etching procedures [23-26]. Thus, this is the first time these optical techniques are used to analyze the structural strain in porous GaN prepared by a bottom-up technique such as CVD. The residual tensile strain we observed in the samples is reduced for increasing deposition time, as the nanoporous layer becomes thicker. Additionally, spectrally resolved CL measurements permit to reveal the increase of the NBE emission with respect to the donor

acceptor pair (DAP) band for increasing deposition time, which allows providing qualitative information about the density of the nanoporous GaN layer.

Experimental and samples

Unintentionally doped *n*-type nanoporous GaN films were epitaxially grown by CVD through the direct reaction between metallic Ga (99.999%) and NH_3 (>99.98%) in a horizontal tubular furnace Thermolyne 79300 on substrates composed by 1 μm thick *p*-type GaN (0001) / 3 μm thick undoped GaN (0001) / sapphire (0001). Details on the synthesis procedure have been provided elsewhere [18]. Resuming, the substrates were placed downwards on a BN support at 1.7 cm above the Ga source. The quartz tube was degassed to a pressure below 10^{-2} Torr. Ammonia was introduced into the quartz tube via a mass-flow controller at a settled flow rate of 75 sccm, the pressure in the chamber was kept at 15 Torr and the furnace was heated up to 1203 K, then three different deposition times: 15, 30 and 60 min, under a constant NH_3 flow and pressure were used. The deposition was stopped by shutting down the NH_3 flow and the furnace heating system, leading to cooling it down to room temperature at a pressure of 10^{-2} Torr.

Morphological characterization of the samples was carried out using a JEOL JSM 6400 Scanning Electron Microscope (SEM) operating at 15 kV.

CL spectra were recorded at 80 K with a Gatan MonoCL2 system equipped with a Peltier cooled charge-coupled-device (CCD) detector. The CL system was attached to a LEO 1530 field emission scanning electron microscope (FESEM). The acceleration voltage of the electron beam was varied between 5 and 10 keV, allowing probing different depths of material.

Micro-PL and micro-Raman spectra were obtained at room temperature and 80 K with a Labram HR800UV Raman spectrometer from Horiba-Jobin-Yvon attached to a metallographic microscope, and equipped with a LN2-cooled CCD detector. Samples were excited with a He-Cd UV laser (325 nm) using 40X UV and 15X UV microscope objectives. The scattered light was collected by the same objective, conforming a nearly backscattering configuration.

Results and discussion

Figure 1 shows typical top view SEM images of the nanoporous GaN layers grown at different deposition times. The SEM images reveal the porosity developed in the samples, with the pores oriented along the *c*-crystallographic axis, perpendicular to the substrate [18]. It can be observed that the average diameter of the pores increases for increasing deposition time. A detailed analysis of the porosity through an image processing analysis was performed using ImageJ software. The SEM images were processed as grey scale 8-bit images, assigning the value 255 to the white contrast part and 0 to the black contrast part of the image and values in between both to define the gray scale. The non-zero pixels (white) were associated with GaN, while the zero pixels were associated with the pores. The images were then filtered and the pixels of the grey scale were converted to either 255 or 0 according to the proximity of the pixel to these extreme numbers. Finally, the pore outline was defined using the *watershed* option of the software. The mean value of the pore size and the percentage of porosity in each sample were evaluated using the processed images using the tool *Analyze particles*, the results are listed in Table 1. As seen from the data analysis, the porosity degree in the samples, within the error bar, does not depend, or only slightly decreases, with the deposition time, while the average diameter of the pores increases. It is worth noting according to the data of table 1, that the error in the determination of the pore size increases with deposition time, whereas the error in the determination of the porosity degree decreases.

Table 1. Pore diameter and porosity degree on nanoporous GaN samples grown at different deposition times.

Deposition time (min)	**Mean diameter of pores** (nm)	**Relative area of pores** (%)
15	146 ± 3	40 ± 7
30	181 ± 14	39 ± 4
60	195 ± 34	35 ± 3

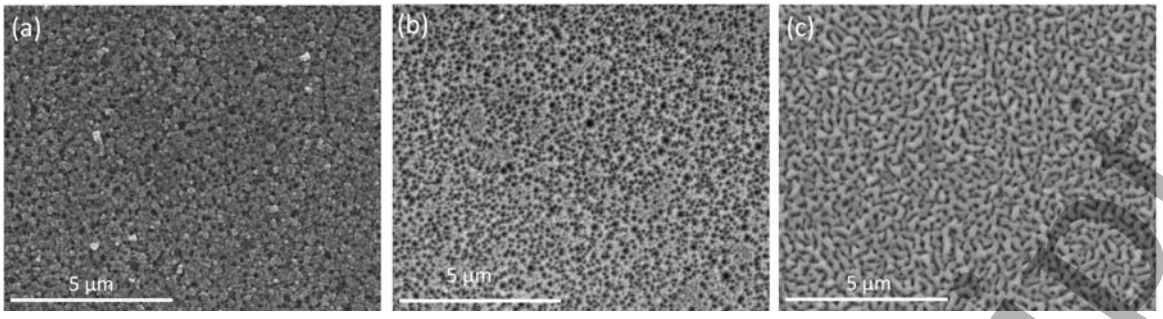

Figure 1. SEM top view images of the nanoporous GaN samples grown at (a) 15, (b) 30, and (c) 60 min

A qualitative perspective of the surface roughness of the epitaxial layers was achieved by recording SEM images with the samples tilted by 60° (see Figure 2). An increase of the surface roughness with the deposition time can be observed. A typical image of the corresponding non-porous GaN substrate exhibiting a smooth surface has been included for comparison (see Figure 2(d)).

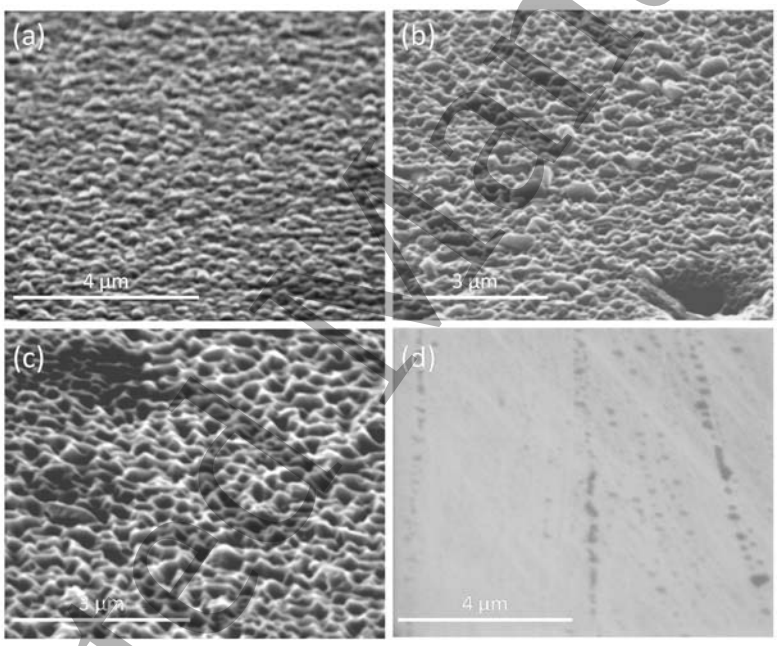

Figure 2. SEM images, tilted by 60°, of nanoporous GaN samples grown at (a) 15, (b) 30, and (c) 60 min. and (d) of the non-porous GaN substrate (for comparison).

Figure 3(a) shows the PL spectra of the nanoporous GaN films recorded at 80 K under excitation with the 325 nm line of a He-Cd laser. The probe depth of the 325 nm light in GaN is ~40 nm [27], which is smaller than the thickness of our epitaxial films [18]. However, due to the porosity of the samples, light might also reach the substrate through the pores, and thus the PL spectra could also contain a contribution from the substrate.

The PL spectra show the NBE emission at around 3.45 eV (360 nm), a donor-acceptor pair (DAP) transition band at 3.28 eV (378 nm) and the DAP-LO phonon replicas separated by the LO phonon energy ~90 meV. The first and the second DAP-LO phonon replicas are seen in the spectra shown in Figure 3(a). Also, in some cases the typical yellow luminescence (YL) band arising from the *n*-type GaN can be observed; this band is mainly associated with Ga vacancies (V_{Ga}) and related complexes [28]. Their presence in the spectra seems to be influenced by the excitation conditions used, especially the penetration depth of the excitation beam, which is particularly difficult to define in porous materials. Thus, their absence in the spectra of some of the samples cannot be considered a probe of the quality of the material, and for that, we did not consider this YL band in our analysis. The NBE emission band in *n*-type GaN is the emission due to neutral donor bound exciton and free exciton transitions, D^0X and FX_A, respectively [29]. At the measurement temperature of 80 K, FX_A is more intense than D^0X, since D^0X is thermally quenched due to the ionization of the neutral donor [30]. Thus, we can assume that the peak labelled as the NBE emission is mainly contributed by the FX_A transition.

The intensity of the NBE band increases with respect to the DAP emission intensity for increasing deposition time. The DAP emission arises from the *p*-type non-porous GaN substrate doped with Mg. The NBE emission, instead, should arise from the unintentionally doped *n*-type nanoporous GaN layer, since the *p*-type substrate does not present the NBE emission, as can be seen in the spectrum obtained for the bare substrate, also included in Figure 3(a). In fact, the NBE band in Mg-doped GaN is usually quenched [31]. As the thickness of the nanoporous layer increases with the deposition time [18] one observes the NBE band to be enhanced, while the DAP emission and its phonon replicas are simultaneously quenched due to the reduced contribution of the substrate in thicker porous layers. However, it is difficult to analyse how the intensity of the NBE band is affected by the structural factors. From one side the porosity present in our samples makes difficult to determine exactly the probed volumes in the sample. From another side, the deposition temperatures used might allow Mg acceptors diffuse during growth towards the growing porous layers [32] [33] creating a transition layer at the interface. Despite in previous studies of deposition of Mg-doped porous GaN layers on already porous undoped GaN samples [18] we did not observe such dopant diffusion, we cannot rule out this hypothesis.

The peak energy of the NBE band as a function of the deposition time is plotted in Figure 3(b). As the deposition time increases, the NBE band shifts towards the high energy side, from 3.432 eV (361 nm) for a deposition time of 15 min, to 3.467 eV (357 nm) for a deposition time of 60 min. As previously discussed, the energy gap of a semiconductor is affected by the residual strain [7]. When GaN is under tensile strain, the NBE emission is shifted towards lower energies, while compressive strain leads to a blue-shift of the NBE. Compared to the position of the NBE emission in a strain free ideal GaN sample, which the FX_A emission at 80 K peaks at 3.47 eV [34], one can argue that our samples are under tensile strain. However, when the thickness of the nanoporous layer is increased, the NBE peak energy approaches the strain free value accounting for strain relaxation for the samples grown for long deposition times. One could consider that the blue shift observed with increasing layer thickness might be associated with the presence of free carriers in the top part of the thick nanoporous layers, due to the Burstein-Moss effect [35]. However, this effect must be negligible here, since we have shown previously that the carrier concentration of an unintentionally doped *n*-type nanoporous GaN grown by CVD was $\sim 10^{16}$ cm^{-3} [18]. At this concentration the Burstein-Moss shift is almost negligible. Thus, these results indicate a reduction in the structural strain in the samples as the deposition time increases.

The shape of the observed DAP related peaks changes between the different samples. The lineshape of this band depends on the concentration of Mg, as a consequence of the complexity of the Mg acceptor configuration in the GaN lattice [36], and the difficulty to set up the conditions for the optimum Mg doping. Recently, different DAP transitions associated with three different Mg-related acceptor levels have been reported [37]. Thus, the shape of the DAP band depends on the relative intensity of these three DAP transitions and it can substantially differ from the shape of a standard DAP peak with its corresponding phonon replicas. This band can even appear energetically shifted depending on the Mg concentration and the dominant DAP transition. Additionally, long-range potential fluctuations have been reported in Mg-doped GaN, which can also contribute to change the shape of the DAP band [36, 38]. This can explain the differences of the DAP band for the different samples studied. The differences in the DAP band shape observed between ours porous GaN layers and the p-type substrate seems to suggest the incorporation of Mg acceptors in the lower part of the porous layer that would diffuse from the substrate as a consequence of the deposition temperature used as pointed out before [32, 33].

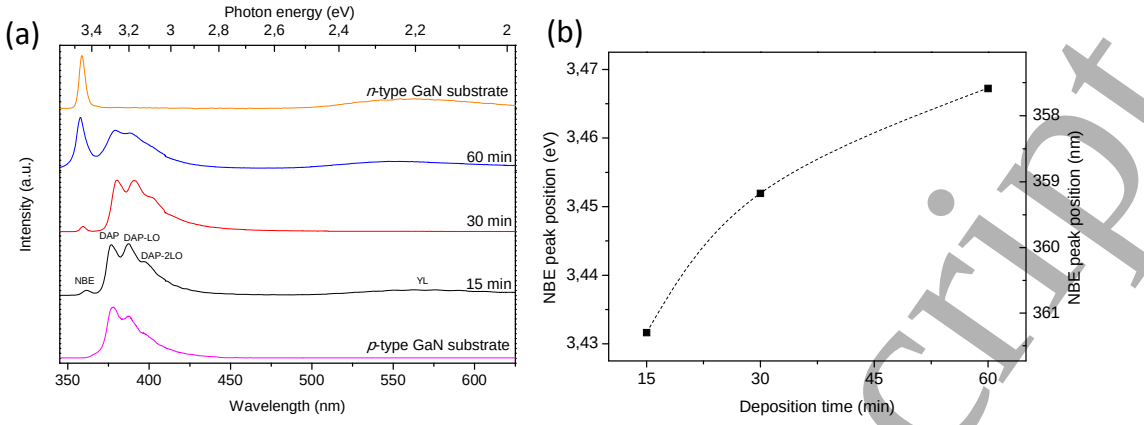

Figure 3. (a) PL spectra recorded at 80 K for nanoporous GaN samples grown at 15, 30 and 60 min. The spectrum of the non-porous *p*-type substrate on which the nanoporous layer are grown is also included. (b) Evolution of the position of the NBE band against the deposition time.

Panchromatic CL (pan-CL) images of the nanoporous GaN samples were recorded. Figure 4 shows a superposition of the SEM image and the corresponding pan-CL image of the sample grown at 30 min. recorded for the same area, in which we changed the degree of transparency of the pan-CL image from 100% transparent to fully opaque to show the correspondence between the pores and the brightest light emission spots. For a better clarity in this sequence, we inverted the contrast of the pan-CL image, i.e., the darkest parts correspond to the regions in which the emission of light is more intense, while the bright parts correspond to regions where the emission of light is poor. In order to guide the reader allowing an easier visualization of the correspondence between the pores and the bright emission spots, some of them have been marked with arrows. By comparing Figure 4(a), corresponding to the SEM image, to Figure 4(f), corresponding to the pan-CL image, one can appreciate circularly shaped forms corresponding to the pores. This would mean that the more intense light emission arises from the pores; one can argue that more light can escape the material due to multiple reflections of light on the lateral walls of the pores, accounting for a better light extraction in the presence of pores. In the intermediate sequence of images between Figures 4(a) and (f), one can see that while the shape of a particular pore is blurred as the % of opacity of the pan-CL image increases, it is replaced by a dark spot, associated with the bright emission of light arising from this spot.

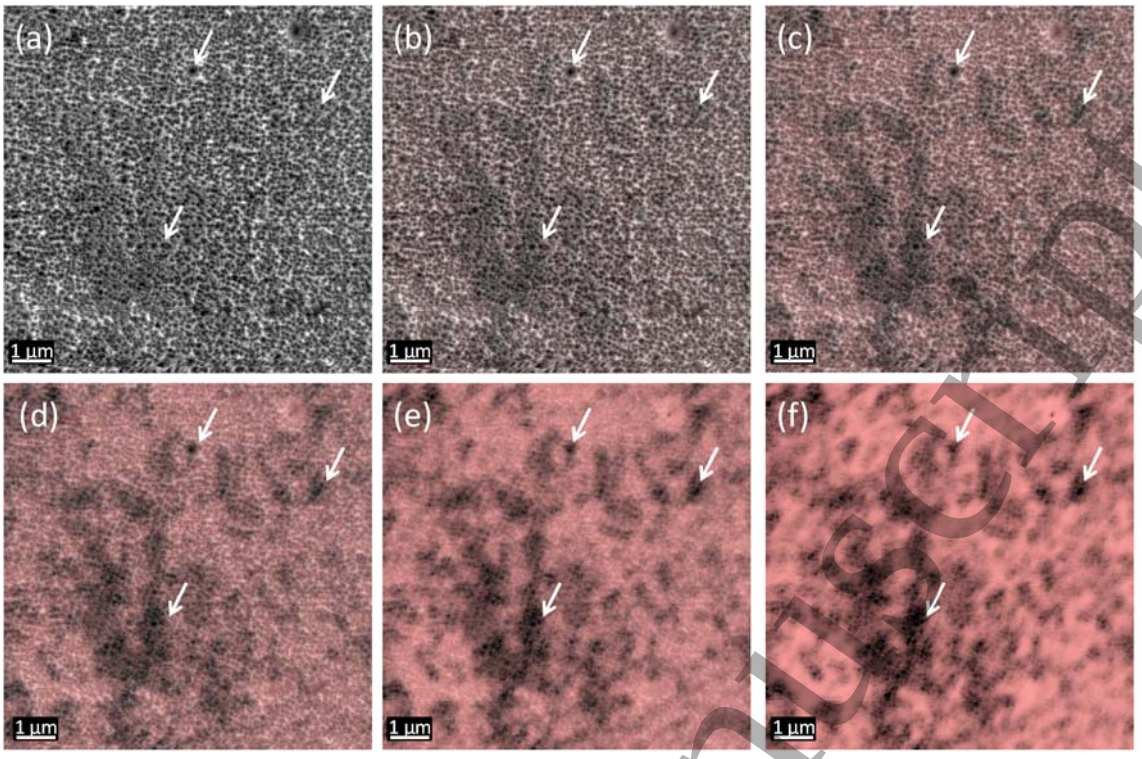

Figure 4. Superposition of SEM and pan-CL images in a sequence going from (a) pure SEM image and adding (b) 20%, (c) 40%, (d) 60%, (e) 80% and (f) 100% of the inverted pan-CL image, where black pixels represent the bright emission light spots of the sample.

The analysis of the CL spectra of the nanoporous GaN samples also confirms the shift of the NBE peak position towards the low energies for decreasing deposition time, corroborating the previous observations done by PL (see Figure 5(a)). This tendency was observed for 5 kV acceleration voltage, for which the CL probe depth in GaN is ≈100 nm, probing the top porous layer. For increasing acceleration voltages, e.g. 10kV, the probe depth is estimated at ≈370 nm. Note that those depths are calculated for bulk GaN; therefore, they must be handled with care when translated to porous layers. The peak energies were 3.398 eV (365 nm), 3.413 eV (363 nm) and 3.435 eV (361 nm) for 15, 30 and 60 min of deposition times, respectively. The differences with the PL energies can be related to the different generation volume in both experiments, and/or to a slight heating by the e-beam; nevertheless, the energy difference shifts between the different samples is preserved for both measurements.

The CL signal arises from the excited generation volume, which depends on the e-beam energy [39]. The higher the acceleration voltage of the electron beam used, the

higher the penetration depth in the material, as the Grün approximation predicts [40]. Based on this, we tried to carry out a qualitative analysis of the nanoporous GaN layer density by CL. This was done by means of the relative intensity of the NBE peak with respect to that of the DAP peak. As discussed above, the NBE peak arises from the unintentionally doped *n*-type nanoporous GaN layer, while the DAP peak and its LO phonon replicas arise from the *p*-type substrate. In fact, Mg doped GaN (p-type) typically exhibits the DAP band with the phonon replicas, and a very weak, almost unappreciable NBE emission. The DAP band structure is determined by the Mg concentration and its electrical activation [31]. According to this, we would expect a decrease of the NBE/DAP intensity ratio as we increase the acceleration voltage, because the emission should mainly arise from the p-type substrate for high e-beam energies. Figure 5(b) plots the NBE/DAP intensity ratio at different acceleration voltages for the different samples analysed. The NBE/DAP intensity ratio increases from 5 kV to 7 kV electron beam voltages; subsequently it decreases for 10 kV. This behaviour appears more obvious for the thicker porous layers corresponding to 60 min. deposition time. This behaviour evidences a complex electron beam penetration across the nanoporous layer, because of the non homogeneous effective density of the porous layer.

Nevertheless, the CL data obtained at different acceleration voltages can provide an idea of the relative density of the nanoporous samples if one compares the results obtained in the different samples. In previous works [18], an approximate value of the thickness of the nanoporous layer was measured using cross section SEM images, obtaining values of 0.5, 1 and 1.7 μm for samples grown during 15, 30 and 60 min, respectively. Using the Grün equation [40], we obtain values of the electron beam penetration for bulk GaN of 110, 200 and 370 nm for acceleration voltages of 5, 7 and 10 kV, respectively. Figure 5(c) plots the CL spectra of the sample grown during 15 min at different acceleration voltages. It can be seen the presence of the NBE peak only for the lowest acceleration voltage. For the sample grown during 30 min, the NBE peak can be observed for the three acceleration voltages used, but with low intensity, as can be seen in Figure 5(d). Only for the sample grown at 60 min (see Figure 5 (e)) the NBE peak can be observed for all the accelerating voltages analysed with a high intensity, but its relative intensity with respect to the DAP band decreases for increasing electron energy. This shows that the upper part of the porous layer of this sample is free of acceptors. The presence of the DAP band even for the lowest electron energy (5keV) is the consequence of the porosity of the layer, which results in an effective density lower than that of the

bulk material. Therefore, the probe depth is substantially higher than the thickness of the porous layer. Note that the nominal thickness of this porous layer is 1.7 µm: taking into account that the Grün electron range in bulk GaN is 370 nm for 10 keV, and that the bare p-type substrate emission is observed for 10 keV excitation, one can assume that the effective density of these nanoporous GaN layers is substantially reduced with respect to the bulk density by a factor around 5.

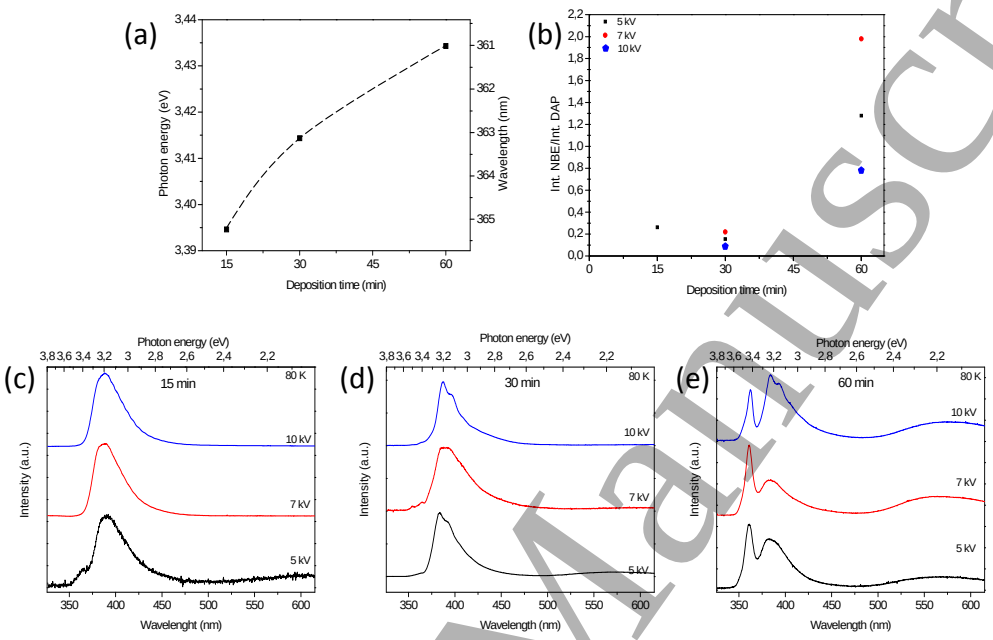

Figure 5. (a) Evolution of the NBE peak position with the deposition time, recorded for an acceleration voltage of 5 kV. (b) Evolution of the intensity ratio between the NBE and DAP emissions with the deposition time at three different acceleration voltages: 5, 7 and 10 kV. CL spectra recorded at these three different acceleration voltages for the samples grown at (c) 15, (d) 30 and (e) 60 min.

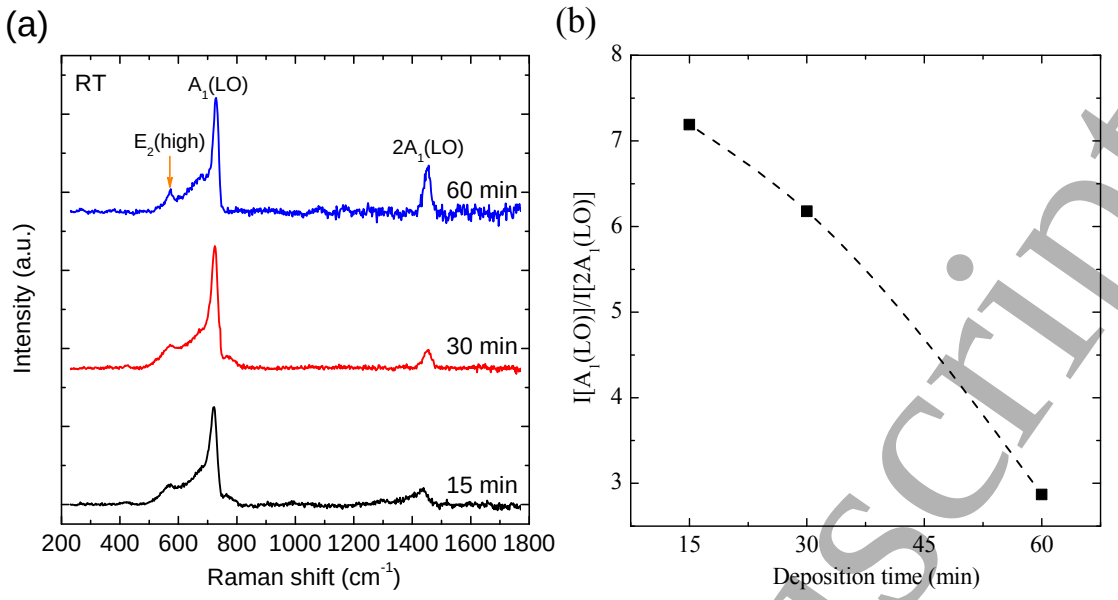

Figure 6. (a) Resonant Raman scattering spectra of nanoporous GaN samples grown at 15, 30 and 60 min excited with a 325 nm laser. (b) Intensity ratio of the $A_1(LO)/2A_1(LO)$ peaks vs deposition time for nanoporous GaN samples.

The results of the resonant Raman scattering under excitation with 325 nm (3.815 eV), above the band gap of GaN, are shown in Figure 6(a) once the background luminescence emission has been subtracted. A strong first order $A_1(LO)$ peak and a second order $2A_1(LO)$ peak with lower intensity can be easily identified in the spectra recorded for the samples grown at different deposition times. The $E_2(high)$ mode can be observed also with a very low intensity, since the non-polar phonons are not resonantly enhanced [13], and the scattering volume for UV in the porous layers is very small.

First, we studied the $E_2(high)$ peak. Peak frequencies of 570, 572, and 574 cm^{-1} were obtained for the samples grown during 15, 30 and 60 min, respectively. These values are always above the frequency reported for the strain-free GaN (568 cm^{-1}) [41]. Thus, this would indicate a contradiction with the data obtained by PL and CL. However, as it can be seen in Figure 6(a), the $E_2(high)$ peak appears as a low intensity, broad, and not well defined peak overlapped by the low frequency broad spectral features associated with the $A_1(LO)$ phonon band, especially for the samples deposited at shorter times, which makes difficult to reliably determine the peak frequency, and therefore, extract from it information about the structural strain. Note, however, that the strain shift of the Raman bands is small, compared with the incertitude of the measurement.

We focus the study in the much better defined polar A_1(LO) phonon. Peak frequencies of 717, 721.3 and 724 cm^{-1} were obtained for the samples grown during 15, 30 and 60 min, respectively. All of them are below the frequency reported for strain-free GaN, which A_1(LO) peak appears at 734 cm^{-1} [42]. However, the A_1(LO) band under resonant conditions is redshifted because of the Martin's double resonance [43]; in fact, the A_1(LO) band in the substrate reference under resonant excitation is observed at 729 cm^{-1}. The Raman shift of the nanoporous samples with respect to the reference cannot be accounted for by strain, because the experimental shift observed would lead to unreasonable strain values [42]. It should be noted that the double Martin's resonance is mediated by charged defects or impurity centres. Furthermore, broad spectral features are observed at both sides of the A_1(LO) band (≈660 cm^{-1} and 760 cm^{-1}), with decreasing intensity from 15 to 60 min deposition times; these broad bands can be associated with defect-activated modes. The FWHM of the A_1(LO) band evolves from 21.5 cm^{-1} for the 15 min deposition sample to 16.7 cm^{-1} for the 60 min deposition sample, which roughly matches the FWHM of the reference substrate. All these data points to a significant improvement of the crystal order in the porous layers for increasing time deposition. Finally, Figure 6(b) represents the A_1(LO)/$2A_1$(LO) intensity ratio vs. deposition time. This intensity ratio decreases as the deposition time increases, indicating the improvement of the crystalline and structural quality of the sample obtained at longer deposition times. This tendency is supported by the evolution of the FWHM of the A_1(LO) peak, indicating that effectively, the concentration of defects is substantially reduced when the deposition time is increased. The presence of those defects would be responsible for the strain deduced from the luminescence measurements in the initial growth stages of the nanoporous layers. The nature of the strain is tensile, which suggests the presence of vacancy complexes.

Conclusions

In summary, we characterized the optical properties of unintentionally doped *n*-type nanoporous GaN grown at different deposition times by CVD. PL has revealed a red-shift of the NBE emission peak for low deposition times that vanishes when the deposition time increases pointing towards a structural relaxation for the samples grown under longer times. CL analysis confirms this tendency from the position of the NBE emission peak. At the same time pan-CL images proved that the brightest emission spots coincide with

the location of the pores, confirming the benefits of the porous layers for the light extraction from the material. Finally, resonant Raman scattering allowed to conclude that the strain suffered from the sample is due to the existence of defects, which are formed in higher concentration at the interface between the substrate and the epitaxial porous layer. The crystalline order is seen to improve for long deposition times, thus, the strain induced at the interface is relaxed. The nature of the strain is tensile, which suggests the presence of vacancy complexes.

Acknowledgements

This work was supported by the Spanish Government under Projects No. TEC2014-55948-R and MAT2016-75716-C2-1-R (AEI/FEDER, UE), and the Catalan Authority under Project No. 2014SGR1358. FD acknowledges additional support through the ICREA Academia awards 2010ICREA-02 for excellence in research. O. Martínez and J. Jimenez were funded by the Spanish Government under projects CICYT MAT2010-20441-C02 (01 and 02) and ENE2014-56069-C4-4-R (MINECO), and Junta de Castilla y León under Projects VA293U13 and VA081U16.

References

[1] Zhang Z-H, Kyaw Z, Liu W, Ji Y, Wang L, Tan S T, Sun X W and Demir H V 2015 A hole modulator for InGaN/GaN light-emitting diodes *Appl. Phys. Lett.* **106** 063501

[2] Nakamura S 1998 The Roles of Structural Imperfections in InGaN-Based Blue Light-Emitting Diodes and Laser Diodes *Science* **281** 956-61

[3] Pearton S J, Kang B S, Suku K, Ren F, Gila B P, Abernathy C R, Jenshan L and Chu S N G 2004 GaN-based diodes and transistors for chemical, gas, biological and pressure sensing *J. Phys.: Condens. Matter* **16** R961

[4] Chen K H, Kang B S, Wang H T, Lele T P, Ren F, Wang Y L, Chang C Y, Pearton S J, Dennis D M, Johnson J W, Rajagopal P, Roberts J C, Piner E L and Linthicum K J 2008 c-erbB-2 sensing using AlGaN/GaN high electron mobility transistors for breast cancer detection *Appl. Phys. Lett.* **92** 192103

[5] Ponce F A, Bour D P, Götz W, Johnson N M, Helava H I, Grzegory I, Jun J and Porowski S 1996 Homoepitaxy of GaN on polished bulk single crystals by metalorganic chemical vapor deposition *Appl. Phys. Lett.* **68** 917-9

[6] Park B-G, Saravana Kumar R, Moon M-L, Kim M-D, Kang T-W, Yang W-C and Kim S-G 2015 Comparison of stress states in GaN films grown on different substrates: Langasite, sapphire and silicon *J. Cryst. Growth* **425** 149-53

[7] Kisielowski C, Krüger J, Ruvimov S, Suski T, Ager J W, Jones E, Liliental-Weber Z, Rubin M, Weber E R, Bremser M D and Davis R F 1996 Strain-related phenomena in GaN thin films *Phys. Rev. B* **54** 17745-53

[8] Neugebauer J and Van de Walle C G 1994 Atomic geometry and electronic structure of native defects in GaN *Phys. Rev. B* **50** 8067-70

[9] Hsu S C, Pong B J, Li W H, III T E B, Graham S and Liu C Y 2007 Stress relaxation in GaN by transfer bonding on Si substrates *Appl. Phys. Lett.* **91** 251114

[10] Van de Walle C G 2003 Effects of impurities on the lattice parameters of GaN *Phys. Rev. B* **68** 165209

[11] Wang D, Jia S, Chen K J, Lau K M, Dikme Y, Gemmern P v, Lin Y C, Kalisch H, Jansen R H and Heuken M 2005 Micro-Raman-scattering study of stress distribution in GaN films grown on patterned Si(111) by metal-organic chemical-vapor deposition *J. Appl. Phys.* **97** 056103

[12] Hartono H, Soh C B, Chua S J and Fitzgerald E A 2007 Fabrication and characterization of nano-porous GaN template for strain relaxed GaN growth *physica status solidi (b)* **244** 1793-6

[13] Dhara S, Chandra S, Mangamma G, Kalavathi S, Shankar P, Nair K G M, Tyagi A K, Hsu C W, Kuo C C, Chen L C, Chen K H and Sriram K K 2007 Multiphonon Raman scattering in GaN nanowires *Appl. Phys. Lett.* **90** 213104

[14] Williamson T L, Díaz D J, Bohn P W and Molnar R J 2004 Structure–property relationships in porous GaN generated by Pt-assisted electroless etching studied by Raman spectroscopy *Journal of Vacuum Science & Technology B: Microelectronics and Nanometer Structures Processing, Measurement, and Phenomena* **22** 925-31

[15] Lin C F, Chen K T, Lin C M and Yang C C 2009 InGaN-Based Light-Emitting Diodes With Nanoporous Microhole Structures *IEEE Electron Device Lett.* **30** 1057-9

[16] Nowak G, Xia X H, Kelly J J, Weyher J L and Porowski S 2001 Electrochemical etching of highly conductive GaN single crystals *J. Cryst. Growth* **222** 735-40

[17] Yam F K and Hassan Z 2009 Structural and optical characteristics of porous GaN generated by electroless chemical etching *Mater. Lett.* **63** 724-7

[18] Bilousov O V, Carvajal J J, Mena J, Martínez O, Jiménez J, Geaney H, Díaz F, Aguiló M and O'Dwyer C 2014 Epitaxial growth of (0001) oriented porous GaN layers by chemical vapour deposition *CrystEngComm* **16** 10255-61

[19] Carvajal J J, Bilousov O V, Drouin D, Aguiló M, Díaz F and Rojo J C 2012 Chemical Vapor Deposition of Porous GaN Particles on Silicon *Microsc. Microanal.* **18** 905-11

[20] Bilousov O V, Carvajal J J, Drouin D, Mateos X, Díaz F, Aguiló M and O'Dwyer C 2012 Reduced Workfunction Intermetallic Seed Layers Allow Growth of Porous n-GaN and Low Resistivity, Ohmic Electron Transport *ACS Appl. Mater. Interfaces* **4** 6927-34

[21] Bilousov O V, Geaney H, Carvajal J J, Zubialevich V Z, Parbrook P J, Giguère A, Drouin D, Díaz F, Aguiló M and O'Dwyer C 2013 Fabrication of p-type porous GaN on silicon and epitaxial GaN *Appl. Phys. Lett.* **103** 112103

[22] Bilousov O V, Carvajal J J, Geaney H, Zubialevich V Z, Parbrook P J, Martínez O, Jiménez J, Díaz F, Aguiló M and O'Dwyer C 2014 Fully Porous GaN p–n Junction Diodes Fabricated by Chemical Vapor Deposition *ACS Appl. Mater. Interfaces* **6** 17954-64

[23] Vajpeyi A P, Tripathy S, Chua S J and Fitzgerald E A 2005 Investigation of optical properties of nanoporous GaN films *Physica E: Low-dimensional Systems and Nanostructures* **28** 141-9

[24] Yam F K, Hassan Z, Chuah L S and Ali Y P 2007 Investigation of structural and optical properties of nanoporous GaN film *Appl. Surf. Sci.* **253** 7429-34

[25] Mahmood A, Hassan Z, Yam F K and Chuah L S 2010 Characteristics of undoped porous GaN prepared by UV assisted electrochemical etching *Optoelectronics and Advanced Materials, Rapid Communications* **4** 1316-20

[26] Najar A, Gerland M and Jouiad M 2012 Porosity-induced relaxation of strains in GaN layers studied by means of micro-indentation and optical spectroscopy *J. Appl. Phys.* **111** 093513

[27] Correia M R, Pereira S, Pereira E, Frandon J and Alves E 2003 Raman study of the A1(LO) phonon in relaxed and pseudomorphic InGaN epilayers *Appl. Phys. Lett.* **83** 4761-3

[28] Kamyczek P, Placzek-Popko E, Kolkovsky V, Grzanka S and Czernecki R 2012 A deep acceptor defect responsible for the yellow luminescence in GaN and AlGaN *J. Appl. Phys.* **111** 113105

[29] Cheng K, Degroote S, Leys M, Germain M and Borghs G 2010 Strain effects in GaN epilayers grown on different substrates by metal organic vapor phase epitaxy *J. Appl. Phys.* **108** 073522

[30] Luong Tien T, Lin K L, Chang E Y, Huang W C, Hsiao Y L and Chiang C H 2009 Photoluminescence and Raman studies of GaN films grown by MOCVD *J. Phys. Conf. Ser.* **187** 012021

[31] Hortelano V, Martínez O, Cuscó R, Artús L and Jiménez J 2016 Cathodoluminescence study of Mg activation in non-polar and semi-polar faces of undoped/Mg-doped GaN core–shell nanorods *Nanotechnology* **27** 095706

[32] Köhler K, Gutt R, Wiegert J and Kirste L 2013 Diffusion of Mg dopant in metal-organic vapor-phase epitaxy grown GaN and AlxGa1−xN *J. Appl. Phys.* **113** 073514

[33] Benzarti Z, Halidou I, Bougrioua Z, Boufaden T and El Jani B 2008 Magnesium diffusion profile in GaN grown by MOVPE *J. Cryst. Growth* **310** 3274-7

[34] Slimane A B, Najar A, Elafandy R, San-Román-Alerigi D P, Anjum D, Ng T K and Ooi B S 2013 On the phenomenon of large photoluminescence red shift in GaN nanoparticles *Nanoscale Res. Lett.* **8** 342

[35] Teisseyre H, Perlin P, Suski T, Grzegory I, Porowski S, Jun J, Pietraszko A and Moustakas T D 1994 Temperature dependence of the energy gap in GaN bulk single crystals and epitaxial layer *J. Appl. Phys.* **76** 2429-34

[36] Eckey L, Gfug U v, Holst J, Hoffmann A, Kaschner A, Siegle H, Thomsen C, Schineller B, Heime K, Heuken M, Schön O and Beccard R 1998 Photoluminescence and Raman study of compensation effects in Mg-doped GaN epilayers *J. Appl. Phys.* **84** 5828-30

[37] Callsen G, Wagner M R, Kure T, Reparaz J S, Bügler M, Brunnmeier J, Nenstiel C, Hoffmann A, Hoffmann M, Tweedie J, Bryan Z, Aygun S, Kirste R, Collazo R and Sitar Z 2012 Optical signature of Mg-doped GaN: Transfer processes *Phys. Rev. B* **86** 075207

[38] Reshchikov M A, Xie J, He L, Gu X, Moon Y T, Fu Y and Morkoç H 2005 Effect of potential fluctuations on photoluminescence in Mg-doped GaN *Phys Stat Sol (C)* **2**

[39] Reimer L 1998 *Scanning Electron Microscopy. Physics of Image Formation and Microanalysis*: Springer-Verlag Berlin Heidelberg)

[40] Everhart T E and Hoff P H 1971 Determination of Kilovolt Electron Energy Dissipation vs Penetration Distance in Solid Materials *J. Appl. Phys.* **42** 5837-46

[41] Wieser N, Klose M, Dassow R, Scholz F and Off J 1998 Raman studies of longitudinal optical phonon–plasmon coupling in GaN layers *J. Cryst. Growth* **189–190** 661-5

[42] Demangeot F, Frandon J, Renucci M A, Briot O, Gil B and Aulombard R L 1996 Raman determination of phonon deformation potentials in α-GaN *Solid State Commun.* **100** 207-10

[43] Davydov V Y, Klochikhin A A, Smirnov A N, Strashkova I Y, Krylov A S, Lu H, Schaff W J, Lee H M, Hong Y L and Gwo S 2009 Selective excitation of E1(LO) and A1(LO) phonons with large wave vectors in the Raman spectra of hexagonal InN *Phys. Rev. B* **80** 081204